

Transparent and Solution Processable Low Contact Resistance SWCNT/AZONP Bilayer Electrodes for Sol-Gel Metal Oxide Thin Film Transistor

Su Jeong Lee, Tae Il Lee, Jung Han Kim, Chul-Hong Kim, Gee Sung Chae, Jae-Min Myoung

Abstract—The contact resistance between source/drain electrodes and semiconductor layer is an important parameter affecting electron transporting performance in the thin film transistor (TFT). In this work, we introduced a transparent and the solution processable single-walled carbon nanotube (SWCNT)/Al-doped ZnO nano particle (AZO NP) bilayer electrodes showing low contact resistance with indium-oxide (In_2O_3) sol gel thin film. By inserting low work function AZO NPs into the interface between the SWCNTs and the In_2O_3 which has a high energy barrier, we could obtain an electrical Ohmic contact between them. Finally, with the SWCNT-AZO NP bilayer electrodes, we successfully fabricated a TFT showing a field effect mobility of $5.38 \text{ cm}^2/\text{V}\cdot\text{s}$ at 250°C .

Keywords—Single-walled carbon nanotube (SWCNT), Al-doped ZnO (AZO) nanoparticle, contact resistance, Thin-film transistor (TFT).

I. INTRODUCTION

FLEXIBLE transparent electrode is an essential component for flexible displays, touch screens, smart windows, LCD, OLED and the solar cell. The material for application of transparent electrode should processes suitable electrical characteristics and high optical properties [1]-[4]. Generally, indium tin oxide (ITO) is widely used as transparent electrodes for electronic devices. ITO shows a high optical transmittance and electrical conductivity. Nevertheless, ITO requires high deposition temperature and its mechanical flexibility is limited for application of flexible electronics. Also, indium, one of material consisting ITO, is too expensive [5], [6]. Various materials like Ag metal nanowires network, CNTs, and graphene was considered as the alternative of ITO. These materials are considered to be cost-efficient due to their solution-processability [7]-[9]. Among these materials, Ag nanowires are attracting substantial interest as a transparent conductor material due to their excellent electrical conductivity that is superior to other materials. However, it is a problem that

the Ag nanowires melt and aggregate when heated over 200°C . Therefore, it causes degradation of the electrical characteristics of the transparent electrode [10]. On the contrary, the single-wall carbon nanotubes (SWCNTs) have excellent heat transfer characteristics and high oxidized temperature, mechanical, optical, and electrical properties [11], [12]. However, the high contact resistance between the SWCNTs and the semiconductor deteriorates the performance of electronic devices [13].

In order to solve this problem, we introduce a solution processable single-walled carbon nanotube (SWCNT)/Al-doped ZnO nano particle (AZO NP) bilayer electrode. An Ohmic contact could be formed by the AZO NPs and then the contact resistance was significant reduced. We experimentally investigated the electrical properties of the SWCNT/AZO NP bilayer electrodes and its contact resistance with the indium-oxide (In_2O_3) channel layer. As a result, an Ohmic contact could be formed so that it is possible to reduce the contact resistance and high performance In_2O_3 TFT could be achieved.

II. RESULT AND DISCUSSION

Fig. 1 (a) illustrates a scheme of bottom gate type TFT with the SWCNTs electrodes and the SWCNT/AZO NP bilayer electrodes. A heavily doped p-type Si (100) substrate with a thermally oxidized 300 nm thick SiO_2 layer was used. The substrate was washed using a piranha solution ($\text{H}_2\text{SO}_4:\text{H}_2\text{O}_2 = 3:1$) to remove organic residues. The In_2O_3 aqueous solution for the channel layer was prepared using 0.1 M of indium nitrate hydrate [$\text{In}(\text{NO}_3)_3 \cdot x\text{H}_2\text{O}$] in deionized (DI) water and then purified the polytetrafluoroethylene (PTFE) syringe filters with 0.2 μm pores to filter out impurities before spin coating. The In_2O_3 channel layer was deposited by spin coating at 3000 rpm for 20 s and annealed at 250°C for 2 h [14]. The source and drain electrodes were formed by using the SWCNT/AZO NP bilayer electrodes. 0.1 wt% AZO NPs (Sigma-Aldrich) was dispersed in ethanol by sonication for 1 h.

AZO NPs solution was deposited by spin coating at 2000 rpm for 30 s and annealed at 100°C for 5 min. This coating procedure was repeated 3 times. The SWCNTs (SA-210, Nano Solution Co. Ltd.) were dispersed in DI water with using a surfactant as sodium dodecyl sulfate. The SWCNTs solution was sprayed at 115°C and then rinsing with DI water. The photo lithography and lift-off process were used to define the source and drain electrodes [15]. Finally, 7 nm In_2O_3 film and 100 nm SWCNT/AZO NP bilayers were obtained.

Su Jeong Lee is with the Department of Materials Science and Engineering, Yonsei University, Seoul, Republic of Korea (e-mail: sjlee87@yonsei.ac.kr).

Tae Il Lee is with the College of BioNano Technology, Gachon University, Gyeonggi-do, Republic of Korea (e-mail: t2.lee77@gmail.com).

Jung Han Kim, Chul-Hong Kim, and Gee Sung Chae are with the Research and Development Center, LG Display, Gyeonggi-do, Republic of Korea (e-mail: junghan.kim@lgdisplay.com, chulhong.kim@lgdisplay.com, jevi@lgdisplay.com).

Jae-Min Myoung is with the Department of Materials Science and Engineering, Yonsei University, Seoul, Republic of Korea (corresponding author to provide phone: 82-2-2123-2843; fax: 82-2-365-2680; e-mail: jmmyoung@yonsei.ac.kr).

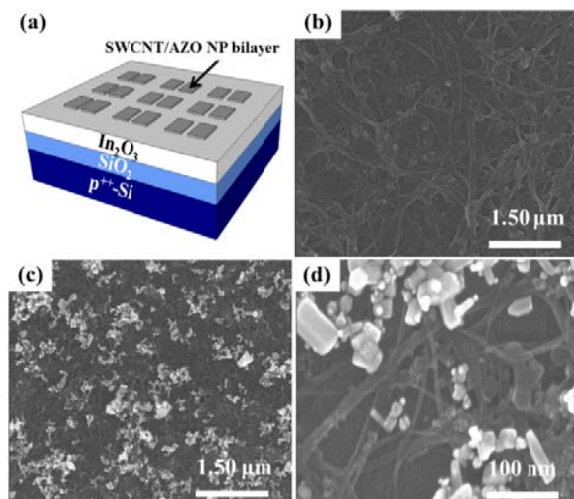


Fig. 1 (a) The SWCNT/AZO NP bilayer electrode TFT. SEM images of (b) SWCNT film and (c), (d) SWCNT/AZO NP bilayer film

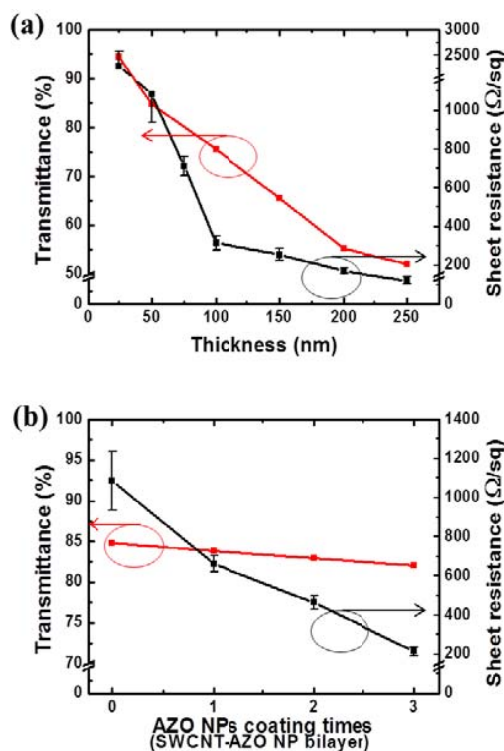


Fig. 2 Characteristic transmittance-sheet resistance curves of (a) SWCNT film as a function of thickness and (b) SWCNT/AZO NP bilayer film as a function of coating times with a thickness of 50 nm

Figs. 1 (b)-(d) show top view field-emission scanning electron microscopy (FESEM, JEOL) images of the SWCNT and the SWCNT/AZO NP bilayer films. The SWCNT film was formed with a random network. The SWCNT film formed well percolation path for the carrier transport, however the small contact area of the SWCNTs with the channel layer interrupted the movement of carriers due to the empty space between the SWCNTs, as shown in Fig. 1 (b). On the other hand, when the

AZO NPs were deposited on the SWCNT film, the contact area of the electrodes increased so that the smooth movement of the carrier was possible, as shown in Figs. 1 (c) and (d).

Fig. 2 shows characteristic transmittance-sheet resistance curves of the SWCNT film and the SWCNT/AZO NP bilayer film as a function of coating times with a thickness of 50 nm. When the SWCNTs thickness increased from 50 to 100 nm, sheet resistance dramatically decreased because interconnecting network formed percolation path between the SWCNTs and the movement of carriers was enhanced. However, the optical transmittance decreased by the increase of the thickness from 94.4 to 58.1%, as shown in Fig. 2 (a), whereas the average transmittance of the SWCNT/AZO NP bilayer film was maintained at 83.4%, as shown in Fig. 2 (b).

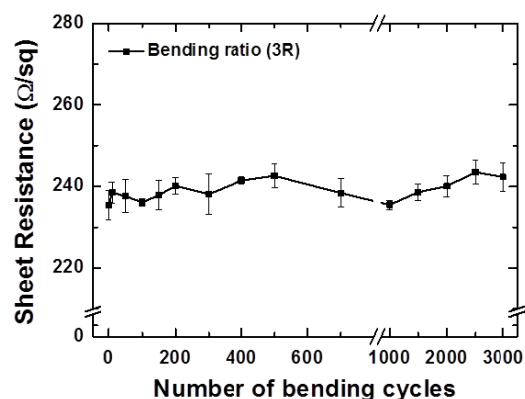


Fig. 3 Variations of the sheet resistance after the bending test of SWCNT/AZO NP bilayer film

Fig. 3 shows the sheet resistance change after the bending test of the SWCNT/AZO NP bilayer film with a radius of curvature of 3 mm. The SWCNT/AZO NP bilayer film was retained stability electrical conductivities during repetitive bending cycles. Moreover, it is notable that the AZO NPs were not removed on the SWCNT film even after 3000 bending cycles.

Fig. 4 shows the electrical contact properties of the SWCNT and the SWCNT/AZO NP bilayer electrodes. To investigate the improvement of the contact resistance in the SWCNT/AZO NP bilayer electrodes, electrical resistance between the channel layer and the electrodes was evaluated by using a transmission line method (TLM).

The TLM patterns from 50 to 250 μm on the In_2O_3 channel layer were formed. Also, the gate voltage increased from 5 to 20 V. The contact resistance ($R_{\text{C}}W$) of the devices was estimated by plotting the width normalized resistance (R_W) as a function of channel length. The intersection at $L=0$ provides the $R_{\text{C}}W$ for each gate voltages [16].

Fig. 4 (a) shows the $R_{\text{C}}W$ value of the SWCNT electrode. The $R_{\text{C}}W$ was changed from 11.5 to 2.62 $\text{M}\Omega$ as a function of channel length. Fig. 4 (b) shows the $R_{\text{C}}W$ value of the SWCNT/AZO NP electrode. The $R_{\text{C}}W$ was changed from 328.4 to 50.6 $\text{K}\Omega$ as a function of channel length. The SWCNT/AZO NP bilayer electrode showed lower $R_{\text{C}}W$ than

that of the SWCNT electrode because AZO NPs reduced the energy barrier height between the SWCNT electrodes and the In_2O_3 channel layer.

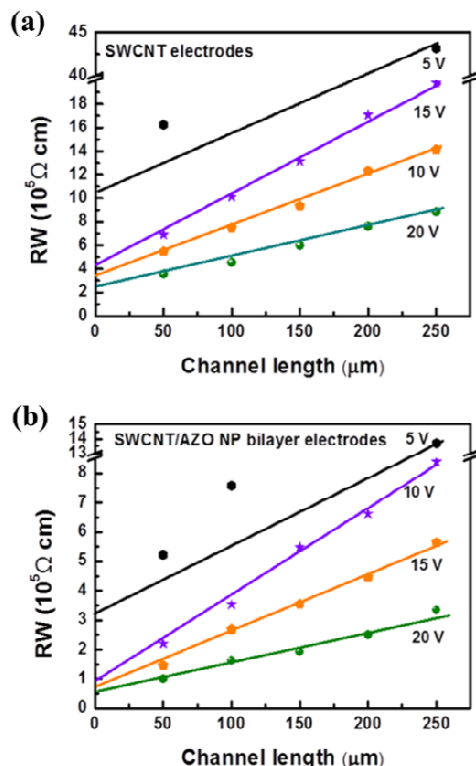


Fig. 4 Width normalized resistance (RW) of the different channel length with different gate voltages (V_{GS}) (a) SWCNT and (b) SWCNT/AZO NP bilayer electrode TFTs

To verify the role of the SWCNT/AZO NPs bilayer electrodes in improving the electrical contact resistance, we fabricated TFTs using SWCNT and SWCNT/AZO NPs bilayer electrode, respectively, and evaluated their electrical performance by using a semiconductor parameter analyzer (Agilent B1500A, Agilent Technologies). Fig. 5 shows transfer and output characteristics of the TFTs with SWCNT and the SWCNT/AZO NPs bilayer electrode, respectively. The channel width was $1000 \mu\text{m}$ and the channel length was $200 \mu\text{m}$, respectively. The saturation field-effect mobility (μ_e) was calculated from [17]

$$I_{DS} = (WC_i/2L) \cdot \mu_{sat} (V_G - V_T)^2 \quad (1)$$

where, C_i is the gate dielectric capacitance per unit area, W is channel width, L is channel length. The threshold voltage (V_{th}) was calculated by linearly fitting the square root of I_{DS} vs V_{GS} . As a result, the μ_e , V_{th} , a sub-threshold slope (S) and I_{on}/I_{off} ratio of SWCNT electrode TFT were measured by $2.93 \text{ cm}^2 \text{ V}^{-1} \cdot \text{s}^{-1}$, -1.36 V , 5.87 V/decade and $\sim 10^3$ at a V_D of 20 V , respectively. And the μ_e , V_{th} , a sub-threshold slope (S) and I_{on}/I_{off} ratio of SWCNT-AZO NP bilayer electrode TFT were $5.35 \text{ cm}^2 \text{ V}^{-1} \cdot \text{s}^{-1}$, 1.52 V , 2.58 V/decade and $\sim 10^4$ at a V_D of 20 V , respectively.

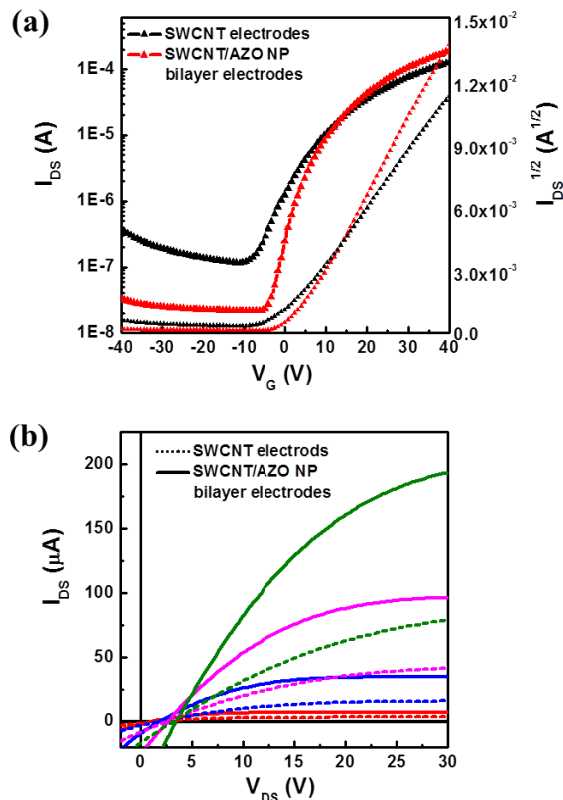


Fig. 5 Electrical characteristics of SWCNTs and SWCNT/AZO NP bilayer electrode TFTs (a) Transfer curves with a V_D of 20 V (b) Output curves with $V_{GS} = 0$ to 40 V in 10 V steps

In summary, a solution processable SWCNT/AZO NP bilayer electrode was introduced. To overcome the high contact resistance of the p-type SWCNTs with n-type In_2O_3 channel layer, the AZO NPs having a low work function was inserted between the SWCNT and the In_2O_3 channel layer. As a result, an Ohmic contact was successfully obtained between source/drain electrodes and channel layer and high performance In_2O_3 TFT could be achieved. This study has a significant technological impact and motivates deeper studies related to the fabrication and characterization of the SWCNT electrode based electronic devices in the aspect of lowering the energy barrier height between the n-type semiconductor and the p-type SWCNT by inserting a low work function conductive NP.

ACKNOWLEDGMENT

This work was supported by the LG Display academic industrial cooperation program.

REFERENCES

- [1] K. A. Sierros, D. S. Hecht, D. A. Banerjee, N. J. Morris, L. Hu, and G. C. Irvin, "Durable transparent carbon nanotube films for flexible device components," *Thin Solid Films*, vol. 518, pp. 6977-6982, 2010.
- [2] S. -K. Chang-Jian, J. -R. Ho, and J.-W. John Cheng, "Fabrication of transparent double-walled carbon nanotubes flexible matrix touch panel by laser ablation technique," *Opt. Laser Technol.*, vol. 43, pp. 1371-1376, 2011.

- [3] S. Hecht, D. Thomas, L. Hu, C. Ladous, T. Lam, Y. Park, G. Irvin, and P. Drzaic, "Carbon-nanotube film on plastic as transparent electrode for resistive touch screens," *Inf. Disp.*, vol. 17, pp. 941-946, 2009.
- [4] W. Fu, L. Liu, K. Jiang, Q. Li, and S. Fan, "Super-aligned carbon nanotube films as aligning layers and transparent electrodes for liquid crystal displays," *Carbon.*, vol. 48, pp. 1876-1879, 2010.
- [5] H. Park, J. S. Kim, B. G. Choi, S. M. Jo, D. Y. Kim, W. H. Hong, and S. Y. Jang, "Sonochemical Hybridization of Carbon Nanotubes with Gold Nanoparticles for The Production of Flexible Transparent Conducting Films," *Carbon.*, vol. 48, pp. 1325-1330, 2010.
- [6] H. L. Peng, W. H. Dang, J. Cao, Y. L. Chen, W. Wu, W. S. Zheng, H. Li, Z. X. Shen, and Z. F. Liu, "Topological insulator nanostructures for near-infrared transparent flexible electrodes," *Nat. Chem.*, vol. 4, pp. 281-286, 2012.
- [7] D. S. Hecht, L. Hu, and G. Irvin, "Emerging Transparent Electrodes Based on Thin Films of Carbon Nanotubes, Graphene, and Metallic Nanostructures," *Adv.Mater.*, vol. 23, pp. 1482-1513, 2011.
- [8] X. Huang, Z. Zeng, Z. Fan, J. Liu, and H. Zhang, "Graphene-Based Electrodes," *Adv.Mater.*, vol. 24, pp. 5979-6004, 2012.
- [9] L. Hu, D. S. Hecht, and G. Grune, "Carbon Nanotube Thin Films: Fabrication, Properties, and Applications," *Chem. Rev.*, vol. 110, pp. 5790-5844, 2010.
- [10] H. H. Khaligh, and I. A. Goldthorpe, "Failure of Silver Nanowire Transparent Electrodes Under Current Flow," *Nanoscale Res. Lett.*, vol. 8, pp. 235, 2013.
- [11] R. L. McCreery, "Advanced Carbon Electrode Materials for Molecular Electrochemistry," *Chem. Rev.*, 2008, vol. 108, pp. 2646-2687, 2008.
- [12] I. Dumitrescu, P. R. Unwin, J. V. Macpherson, "Electrochemistry at Carbon Nanotubes: Perspective and Issues," *Chem. Commun.*, vol. 7345, pp. 6886-7052, 2009.
- [13] J. Jeon, T. I. Lee, J. H. Choi, J. P. Kar, W. J. Choi, H. K. Baik and J. M. Myoung, "Performance Enhanced Carbon Nanotube Films by Mechanical Pressure for a Transparent Metal Oxide Thin Film Field Effect Transistor," *Electrochem. Solid-State Lett.* vol. 14, pp. H76-H79, 2011.
- [14] J. H. Park, Y. B. Yoo, K. H. Lee, W. S. Jang, J. Y. Oh, S. S. Chae, H. W. Lee, S. W. Han, and H. K. Baik, "Boron-Doped Peroxo-Zirconium Oxide Dielectric for High- Performance, Low-Temperature, Solution-Processed Indium Oxide Thin-Film Transistor," *ACS Appl. Mater. Interfaces.*, vol. 5, pp. 8067-8075, 2013.
- [15] J. H. Park, S. J. Lee, T. I. Lee, J. H. Kim, C. H. Kim, G. S. Chae, M. H. Ham, H. K. Baik, and J. M. Myoung, "All-Solution-Processed, Transparent Thin-Film Transistors Based on Metal Oxides and Single-Walled Carbon Nanotubes," *J. Mater. Chem. C*, vol. 1, pp. 1840-1845, 2013.
- [16] G. B. Blanchet, C. R. Fincher, M. Lefenfeld and J. A. Rogers, J. A. "Contact Resistance in Organic Thin Film Transistors," *Appl. Phys. Lett.*, vol. 84, pp. 296-298, 2004.
- [17] B. G. Streetman and S. Banerjee, *Solid State Electronic Devices* 6th edn (Upper Saddle River, NJ: Pearson Education), 2006.